MAUSAM, **73**, 2 (April 2022), 355-364

MAUSAM

DOI : https://doi.org/10.54302/mausam.v73i2.5481
Homepage: https://mausamjournal.imd.gov.in/index.php/MAUSAM

UDC No. 551.579: 551.577.36 (597)

Establishment of flood hazard mapping based on simulating rainfall intensity-duration-frequency curve for the Ca Mau Peninsula of Vietnam

TRUONG AN DANG[#, *]

[#]*University of Science, Ho Chi Minh City, Vietnam*

**Vietnam National University - Ho Chi Minh City, Vietnam*

227 Nguyen Van Cu Str., 5 District, HCM City - 70000, Vietnam

(*Received 27 April 2020, Accepted 25 January 2022*)

e mail : dtan@hcmus.edu.vn

सार – हाल के वर्षों में, मेकांग डेल्टा, वियतनाम के निचले तटीय क्षेत्र (एलसीए) सीए मऊ प्रायद्वीप में अक्सर बाढ़ आई है, जिसमें लोगों के जीवन में कई बाधाएँ उत्पन्न हुई हैं। अत्यधिक वर्षा इस क्षेत्र में बाढ़ का प्रमुख कारण है। इसलिए, वर्षा तीव्रता-अवधि-आवृत्ति (आईडीएफ) मॉडल के अनुकरण के आधार पर वियतनाम के सीए मऊ प्रायंद्वीप के लिए बाढ़ के खतरे के मानचित्रण (एफएचएम) का अध्ययन करना है।

शोध करने के लिए, 1984-2019 की अवधि (बेसलाइन) के लिए क्षेत्र में छह प्रेक्षण स्टेशनों पर दैनिक वर्षा डेटा अनुक्रम और भविष्य के रिप्रेजेन्टेटिव कॉन्सनट्रेशन पाथवे (आरसीपी) आरसीपी 4.5 और आरसीपी 8.5 परिदृश्य 2050 के अनुरूप हैं जिसका उपयोग वर्षा की तीव्रता-अवधि-आवृत्ति मॉडल के लिए किया जाता है। मॉडल परिणामों की मापी गई फील्ड और जारी रिपोर्ट से तुलना करके बाढ़ जोखिम मानचित्रण की विश्वसनीयता का मूल्यांकन किया गया।

परिणाम बताते हैं कि चरम वर्षा की घटनाओं (ईआरई) की विभिन्न अवधियों की तीव्रता अलग-अलग उत्क्रमण के साथ बेसलाइन की तुलना में आरसीपी 4.5 और आरसीपी 8.5 परिदृश्यों के लिए समय के साथ 42.5 और 57.9% तक बढ़ने की संभावना है। सामान्य तौर पर, वर्षा की उच्चतम तीव्रता बेसलाइन के साथ-साथ भविष्य के परिदृश्यों के सभी अलग-अलग वर्षा अंतरालों पर 50 वर्ष के प्रत्यागमन काल में होती है। परिणाम बताते हैं कि बेसलाइन और भविष्य के परिदृश्यों के लिए बाढ़ के खतरे के उप-क्षेत्र पश्चिमी प्रांतों और पूर्वोत्तर प्रांतों के सबसे निचले स्थानों के साथ मेल खाते हैं।

ABSTRACT. In recent years, flooding has frequently occurred in the Ca Mau Peninsula, a low-lying coastal area (LCA) of the Mekong Delta, Vietnam, causing obstacles to many aspects of people's lives. Extreme rainfall is the key cause that led to the flooding of the area. The study, therefore, is to establish flood hazard mapping (FHM) for the Ca Mau Peninsula of Vietnam based on simulating the rainfall intensity-duration-frequency (IDF) model.

To deploy the research, daily rainfall data sequence at six observation stations across the area for the 1984 -2019 period (baseline) and future Representative Concentration Pathway (RCP) RCP4.5 and RCP8.5 scenarios correspond to 2050 timescale is used to simulate the rainfall intensity-duration-frequency model. The reliability of the flood hazard mapping was appraised by comparing the model results to the measured field and issued reports.

The results state that intensities of extreme rainfall events (EREs) various durations with different return periods are all probably to increase over time 42.5 and 57.9% for RCP4.5 and RCP8.5 scenarios compared with baseline. In general, the highest intensity of rainfall occurs at a 50-year return period at all different rainfall intervals of the baseline as well as future scenarios. Results pointed out that the sub-areas of high flood hazard for the baseline and future scenarios coincide with the lowest locations of the western provinces and part of the northeastern provinces.

Key words – Coastal, CumFred software, Flood depth, Global warming, Infrastructures.

1. Introduction

In recent years, natural disasters, such as floods and droughts have expected increasing trends on a global scale and flooding emerges directly from extreme rainfall events (EREs) (Alfieri *et al*., 2015; Courtey *et al*., 2019). Extreme rainfall is valued to be the main cause of flooding, affecting many aspects of life

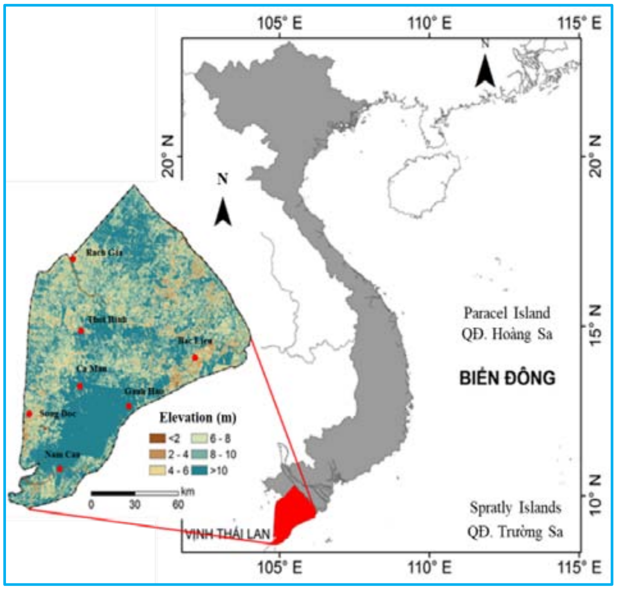

Fig. 1. Map of the study area, with rainfall observation stations marked by red circles (*Source*: Ho and Dang, 2021)

(Skilodimou *et al*., 2021; Termeh *et al*., 2018). They contribute approximately one-third of global hazardous events, and the number of flood incidences has significantly increased over the past few decades (Madsen *et al*., 2014; Ouma and Tateishi, 2014).

Recently, studies indicated that extreme rainfall has recorded an increasing trend in the other regions of Vietnam, leading to flooding for many regions, especially coastal cities (Dang, 2020; Lee and Dang, 2020). Moreover, the most recent report by the Ministry of Natural Resources and Environment (MNRE) (2016) judges that the frequency and magnitude of extreme rainfall events (EREs) across the Mekong Delta will continue to increase in the next decades. This is especially true for the Ca Mau Peninsula, a low-lying coastal area (LCA) of the Mekong Delta have frequently flooded in recent years. A study on flood warnings across the Ca Mau coastal area under the impacts of climate change (ICC) by Dang (2020) indicated that the area has experienced a significant upward in extreme rainfall over the past three decades. For example, an EREs on 9 October 2019, has been prolonged heavy rainfall, thunderstorms, causing local flooding in many places of the Ca Mau Peninsula. Agricultural production, navigation and irrigation works were also seriously affected(Dang, 2020). According to Komolafe *et al*. (2018), the fast-urbanization processes in many municipalities, replacing vegetation with concreted soil surfaces which impede the store's sizable amounts of rainfall, caused by the decrease in soil surface permeability, resulting in the surface runoff peaks will increase quickly in the LCAs. IPCC (2019) notified that the frequency and severity of EREs in the LCAs are strongly affected by flooding depth in the context of climate variability (CCV).

As a consequence of global warming, the climate parameters have been recognized in increasing trends of drought, EREs and flooding (David *et al*., 2020; Feloni *et al*., 2020). Studying the potential changes in the EREs is enhancing one of the most important practical interests for engineering design (Tsanakas *et al*., 2016; Radwan *et al*., 2019). The intensity-duration-frequency (IDF) curve relationship of the rainfall extremes is commonly epitomized as a useful tool for understanding the characteristics of EREs (Bathrellos *et al*., 2017; Ouma and Tateishi, 2014). However, issued studies on IDF are commonly based on observational rainfall data and these curves are rarely updated until new observations are available. According to Bathrellos *et al*. (2017), the simulation of IDF relies on an assumption of rainfall series stationarity that the intensity and frequency of EREs remain unchanged over time. In fact, such assumptions may not be appropriate in the CCV.

Therefore, in this study, the rainfall data for baseline and future conditions will be applied to simulate the IDF curve across the study area. Specifically, the study will focus on the Ca Mau Peninsula, Vietnam. We first appraise the quality of the rainfall data sequence at observation stations across the entire study area based on Buishand's range test. The generalized extreme value (GEV), Gumbel or Pearson Type III function are evaluated before applying them to the rainfall IDF curve simulation under current climate conditions and future scenarios. The projection lasts in the 36-year (1984-2019) for baseline and future corresponds to timescale 2055s (2046-2065) of RCP4.5 and RCP8.5 scenarios. The simulated results of rainfall annual extremes for the baseline are compared with the issued reports to validate the performance of the CumFred model simulation. Finally, the rainfall projections for the baseline and future scenarios are applied to simulate rainfall IDF curves and towards to establish flood hazard mapping across the study area.

2. Materials and method

2.1. *Study area*

Ca Mau Peninsula is located in the southeast of the Mekong Delta, Vietnam, which lies between 8°33'36"-10°19'12" N latitude and 104°42'36"-106°14'24" E longitude including part of Kien Giang Province, Can Tho City and the provinces of Ca Mau, Bac Lieu, Soc Trang and Hau Giang (Fig. 1).

TABLE 1

Description of basic statistical characteristics of averageannual rainfall (AAR) and standard deviation (SD) across study area in the 1984-2019 period

No.	Station	Longitude (E)	Latitude (N)	AAR (mm)	SD (mm)	Period (year)
1.	Bac Lieu	105.72	9.28	1949	299.8	1984-2019
2.	Ganh Hao	105.42	9.03	1885	278.5	1984-2019
3.	Ca Mau	105.15	9.18	2356	311.7	1984-2019
4.	Nam Can	105.07	8.75	2339	289.4	1984-2019
5.	Thoi Binh	105.09	9.35	2337	276.9	1984-2019
6.	Rach Gia	105.07	10.00	2168	356.2	1984-2019

TABLE 2

Change in rainfall compared to the current climate condition according to RCP4.5 and RCP8.5 scenarios at observation stations across the study area

No.	Station	Current climate (mm)	RCP4.5 scenario (mm)	Change (%)	RCP8.5 scenario (mm)	Change (%)
1.	Bac Lieu	1949.2	2164.2	+11.0	2271.4	+16.5
2.	Ca Mau	2356.4	2492.6	+5.8	2610.4	+10.8
3.	Ganh Hao	1885.7	2092.8	+11.0	2196.5	+16.5
4.	Nam Can	2339.1	2474.9	+5.8	2591.9	+10.8
5.	Rach Gia	2168.5	2367.6	+9.2	2480.3	+14.4
6.	Thoi Binh	2337.8	2472.7	+5.8	2589.6	+10.8
	Average	2185.3	2344.2	+8.1	2456.7	+13.3

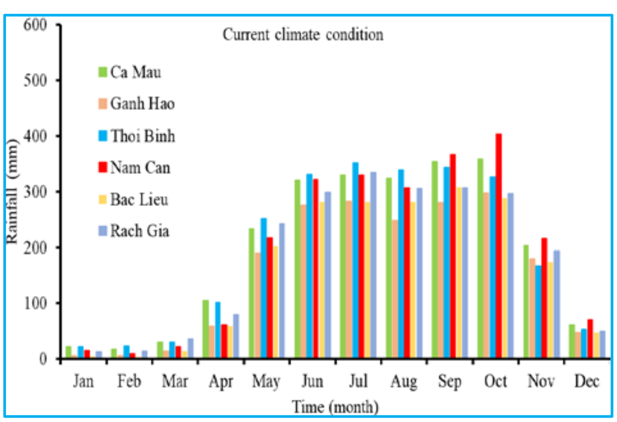

Fig. 2. Rainfall distribution at stations across the study area in the 1984-2019 periods

The key reason for selecting Ca Mau Peninsula for a study area was the fact that it is the LCA and deputizes Vietnam's most vulnerable region to climate change with an elevation varying from 0.5 to 1.5 m above average sea level and partially urbanized catchment characterized by high intense rainfall (Table 1) and the area has recently experienced flooding and significant land subsidence in recent years (Dang, 2020).

Through preliminary analysis, the average annual rainfall across the area varying from 1885 mm at Ganh Hao station to 2356 mm at Ca Mau station (Table 1). The climate is dominated by the tropical monsoon circulation with high-intensity rainfall compared to other provinces in the entire Mekong Delta, with around 90% falls in the

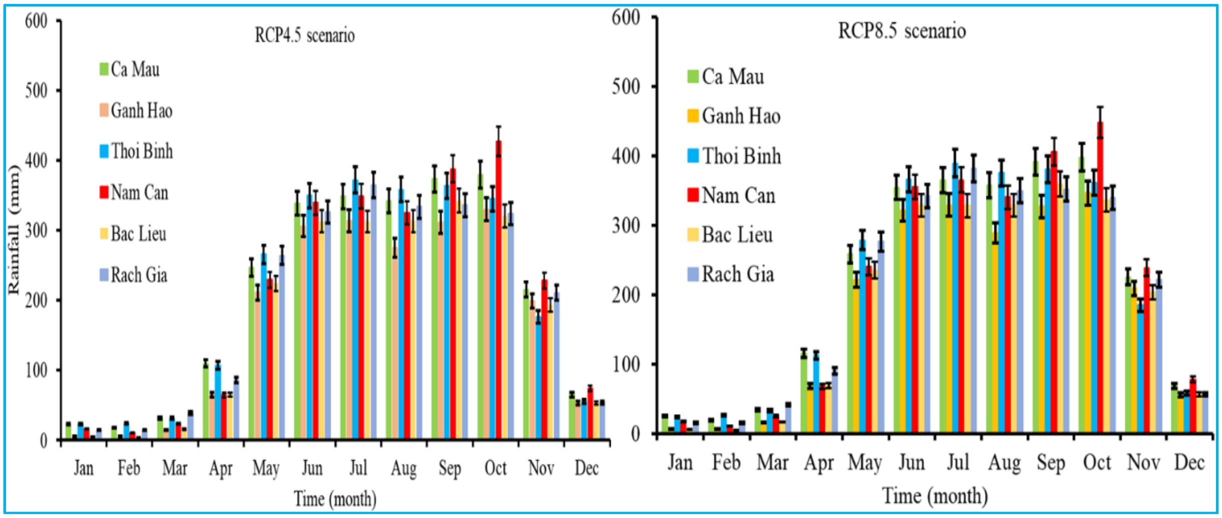

Fig. 3. Changes in rainfall for RCP4.5 and RCP8.5 scenarios (percentage error bars)

rainy season from May to November. The area has a deep divergence of rainfall depending on seasonal and intensity (Fig. 2).

2.2. *Rainfall data collection*

In this study, rainfall data sequence at 6 observation stations across the Ca Mau Peninsula were obtained from the National Centre for Hydro-meteorological Forecasting (NCHF) in the 1984-2019 period was used to simulate the IDF depth, while rainfall data changed corresponds to 2050 timescale of RCP4.5 and RCP8.5 scenarios were consulted from the latest updated report on emission scenarios from regional climate modelling of MNRE (Fig. 3, Table 2).

According to the latest update report of MNRE (2016) on future change scenarios for the Ca Mau Peninsula in the middle stage of the century, the AAR increases compared to the baseline by 5.8-11.0% for the RCP4.5 scenario and 10.8-16.5% for the RCP8.5 scenario (Table 2).

2.3. *Rainfall sequence quality appraisal*

To simulate flooding depth, first, the rainfall data sequence at 6 observation stations across the Ca Mau Peninsula for the 1984-2019 period was arranged into an increasing time series applying R software. Second, the rainfall data sequence at all observation stations was appraised using Buishand's range test. Buishand's range test is constructed by Buishand (1982) to detect the break in the midpoint of any data sequences. The adjusted partial sum (S_k), that is the cumulative deviation from the average value for k^{th} observation of a data series y_1, y_2, y_3, …. y_n with $(\bar{y})$ is an average value of observation data series and can be calculated using the formula:

$$S_k^* = \sum_{i=1}^{k} (y_i - \bar{y}), k = 1,\ldots,n \qquad (1)$$

In this study, Buishand's range test was applied to detect the inhomogeneity of rainfall data sequence at all observation stations across the study area for the 1984-2019 period at a 95% significant level. Therefore, if the *p*-value from any rainfall observation station is smaller the α-value rainfall data sequence will be considered as inhomogeneous (Ho and Dang, 2021).

2.4. *Rainfall IDF depth simulation model*

To define the short time-interval from daily rainfall data, an empirical conversion formula is sorted as Eqn. (2).

$$R_t = R_{24}\sqrt[3]{\frac{t}{24}} \qquad (2)$$

where, R_t is the rainfall amount at hour time-interval, R_{24} is the rainfall amount at daily-interval and t is the lasting intervals of rainfall events.

To simulate the rainfall IDF depths, rainfall data sequence at 6 observation stations corresponding to different durations (varying from 15 to 720 min) is clarified applying cumulative distribution function (CDF). The maximum rainfall intensity corresponding to each

TABLE 3

Results of the rainfall data sequence appraised based on Buishand's range test

No.	Station	α-value	p-value	Results
1.	Bac Lieu	0.05	0.483	homogeneous
2.	Ganh Hao	0.05	0.734	homogeneous
3.	Ca Mau	0.05	0.594	homogeneous
4.	Nam Can	0.05	0.527	homogeneous
5.	Thoi Binh	0.05	0.684	homogeneous
6.	Rach Gia	0.05	0.876	homogeneous

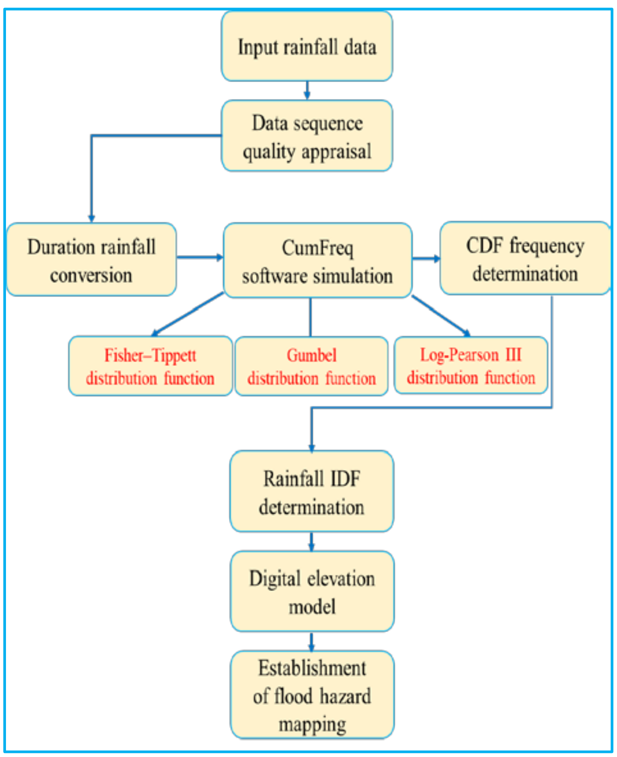

Fig. 4. The flow chart of steps in the process of establishing the flood hazard mapping

interval is related to return periods obtained from the CFD. The maximum cumulative frequency, duration and intensity of rainfall can be simulated by applying generalized extreme value (GEV). A probability distribution will be adopted from the extreme value distributions Gumbel, Pearson types I, II and III and Fisher-Tippett types I, II and III functions. The cumulative frequency, duration, and extreme rainfall intensity, therefore, can be obtained using a distribution function. The cumulative distribution function [$F(x)$] is calculated by Eqn. (3)

$$F(x) = \exp\left\{-\left[1 + k\left(\frac{x-\mu}{\sigma}\right)\right]^{-\frac{1}{k}}\right\} \quad (3)$$

where, μ, σ and ξ are the parameters that represent location, scale, and shape, respectively.

The location parameter is calculated by Eqn. (4)

$$\mu(t) = \mu_1 t + \mu_0 \quad (4)$$

In Eqn. (4), t is time while μ_1 and μ_0 present the intercept and slope parameters, respectively.

For maximum rainfall data sequence, the time-variant parameter [$m(t)$] is obtained by calculating the 95th significant level μ (t). The model parameters will then be applied to simulate the rainfall intensity.

$$q_p = \left[\left(-\frac{1}{\ln p}\right)^{\delta} - 1\right] \times \frac{\sigma}{\delta} + \tilde{\mu}(\delta \neq 0) \quad (5)$$

where, p is frequency, and the n-year rainfall intensity refers to the annual maximum rainfall of specified depth/intensity and duration having a probability of exceedance of 1/n. In this way, rainfall intensity is impressed as a function of the return period and the average length of time between rainfall events of a given intensity and duration.

TABLE 4

Analysis results between the calculated and observed frequencies of the distribution functions by Cum Freq software

No.	Station	Distribution function		
		Gumbel	Pearson	Fisher–Tippett
1.	Bac Lieu	2.62	2.78	2.86
2.	Ca Mau	1.97	2.22	1.99
3.	Ganh Hao	3.05	3.99	3.21
4.	Nam Can	2.96	3.07	3.24
5.	Thoi Binh	1.82	1.89	1.87
6.	Rach Gia	2.38	3.49	2.57
Basic statistical characteristics				
	Max.	3.05	3.99	3.24
	Min.	1.82	1.89	1.87
	Ave.	2.46	2.90	2.62

TABLE 5

Frequency analysis results for daily rainfall correspond to various return periods of the baseline period and RCP4.5 and RCP8.5 scenarios

Station	Frequency distribution function	Daily rainfall at various return periods (hr)								
		0.25	0.5	1.0	1.5	2.0	3.0	5.0	8.0	12.0
Baseline period										
Bac Lieu	Gumbel	153.7	96.6	60.4	46.8	38.7	29.5	18.6	15.5	11.4
Ca Mau	Gumbel	133.4	83.6	52.5	40.7	33.8	25.6	16.5	13.7	10.9
Ganh Hao	Gumbel	153.1	95.4	60.8	45.5	37.6	28.9	18.5	15.8	11.4
Nam Can	Gumbel	164.5	103.4	65.7	49.5	41.4	31.5	19.8	16.2	12.8
Rach Gia	Gumbel	148.7	94.3	59.5	45.4	37.5	28.6	18.0	14.9	11.8
Thoi Binh	Gumbel	106.3	67.0	42.5	32.8	26.7	20.9	12.7	10.8	8.9
RCP4.5 scenario										
Bac Lieu	Gumbel	218.5	135.7	97.2	62.8	51.8	41.8	27.4	21.5	16.8
Ca Mau	Gumbel	187.9	116.2	75.9	61.1	47.8	36.7	24.5	18.9	15.7
Ganh Hao	Gumbel	217.6	146.8	88.7	70.9	61.1	45.6	28.7	23.7	18.8
Nam Can	Gumbel	252.4	171.5	101.9	82.8	68.7	52.9	33.8	27.9	20.7
Rach Gia	Gumbel	201.8	121.9	78.9	64.7	54.2	41.8	26.2	20.6	16.5
Thoi Binh	Gumbel	147.5	99.8	60.8	49.8	41.1	31.1	18.9	16.8	12.9
RCP8.5 scenario										
Bac Lieu	Gumbel	245.5	151.9	94.9	69.7	65,1	44.9	29.8	24.2	16.4
Ca Mau	Gumbel	209.8	130.7	78.8	59.7	56,5	37.8	24.9	20.7	15.2
Ganh Hao	Gumbel	242.6	151.8	92.4	68.7	64,3	43.5	30.1	22.1	17.8
Nam Can	Gumbel	264.7	164.9	103.4	75.2	69,6	48.6	31.6	25.7	18.9
Rach Gia	Gumbel	227.6	141.7	83.7	64.3	61,0	41.7	27.4	20.9	16.9
Thoi Binh	Gumbel	167.8	104.3	63.5	48.6	45,2	30.9	20.5	15.1	12.5

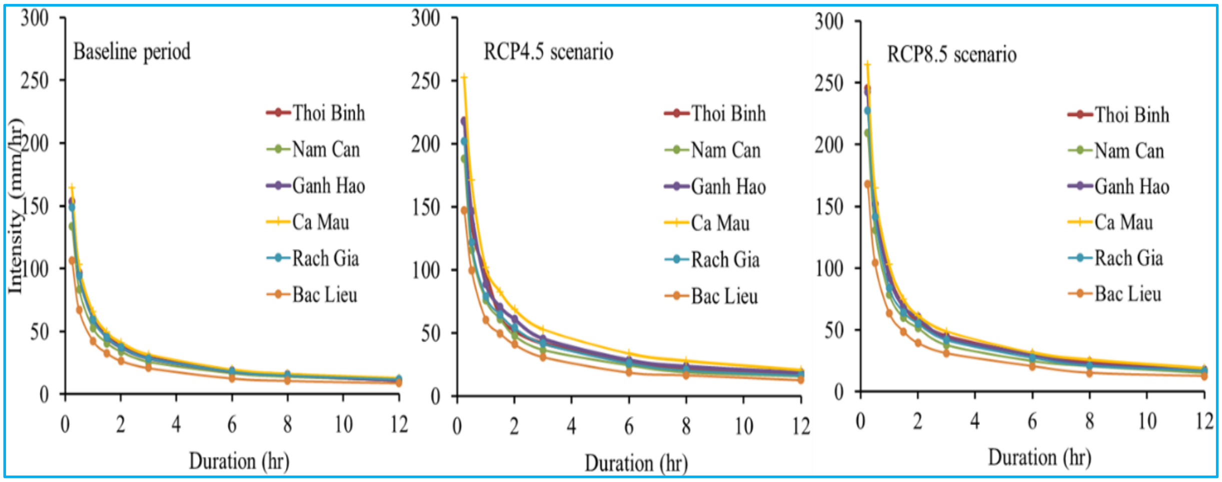

Fig. 5. Projected rainfall intensity for the Ca Mau Peninsula under the baseline period and future periods scenarios correspond to various durations (*i.e.*, 0.25, 0.5, 1.0, 1.5, 2.0, 3.0, 5.0, 8.0 and 12.0 h) with return period 50-year return period

A detailed process of the establishment of flood hazard mapping based on simulating rainfall IDF depth is given in Fig. 4.

3. Results and discussion

3.1. *Rainfall data sequence quality*

The rainfall data sequence quality at all observation stations across the study area in the 1984-2019 period is appraised based on Buishand's range test. The rainfall data sequence is rated to be homogeneous if the null hypothesis is accepted with the obtained *p*-values larger than the significance level of α. Results point out that at a 95% significant level, the values of *p* in Buishand's range test reach from 0.483 to 0.876, respectively (Table 3). Table 3 shows that the critical values of p are more than the significance level of α, which is synonymous with the rainfall data sequence quality applied for the study area being homogeneous.

3.2. *Analysis results of the GEV distribution function*

The analysis of the maximum 1-day cumulative frequency of rainfall shows the correlation between the actual and calculated cumulative frequency rainfall from the applied distribution functions. Based on the findings, the Gumbel function has the lowest mean deviation compared to Pearson and Fisher-Tippett functions (Table 4). Specifically, results show that average, maximum and minimum values of the Gumbel function are 2.46, 3.05 and 1.82, respectively while corresponding values of Pearson and Fisher-Tippett functions are 2.90, 3.99, 1.89 and 2.62, 3.24, 1.87, respectively. Results imply that the Gumbel distribution function obtains the best simulation results, and the Gumbel distribution function is, therefore, selected for rainfall IFD depth simulation in this case study.

3.3. *Rainfall intensities*

Results show that the extreme rainfall intensity at the 50-year return period at all observation stations ranged from 106.3 to 164.5 mm hr^{-1} for short-duration rainstorms (15 min) of baseline while corresponding values range from 167.5 to 252.4 mm hr^{-1} and from 167.8 to 264.7 mm hr^{-1}, respectively for RCP4.5 and RCP8.5 scenarios (Table 5).

Specifically, for the durations from 60 to 720 hr, the maximum rainfall intensities at the 50-year return period at recorded 164.5 mm hr^{-1} for baseline while the corresponding values of RCP4.5 and RCP8.5 scenarios simulated up to 252.4 and 264.7 mm hr^{-1}, respectively at Nam Can station (Fig. 5). A similar study result for Central Vietnam by Thanh and Remo (2018) confirmed that the EREs are expected to frequently increase under the ICV.

3.4. *Flood hazard mapping analysis*

In recent years, the Ca Mau Peninsula is undergoing rapid subsidence, along with a fast urbanization process and rising seawater level, leading to increased flooding areas. It is, therefore, essential to establish the flood hazard mapping for the entire study area, contributing to minimizing negative impacts on people's lives. Two

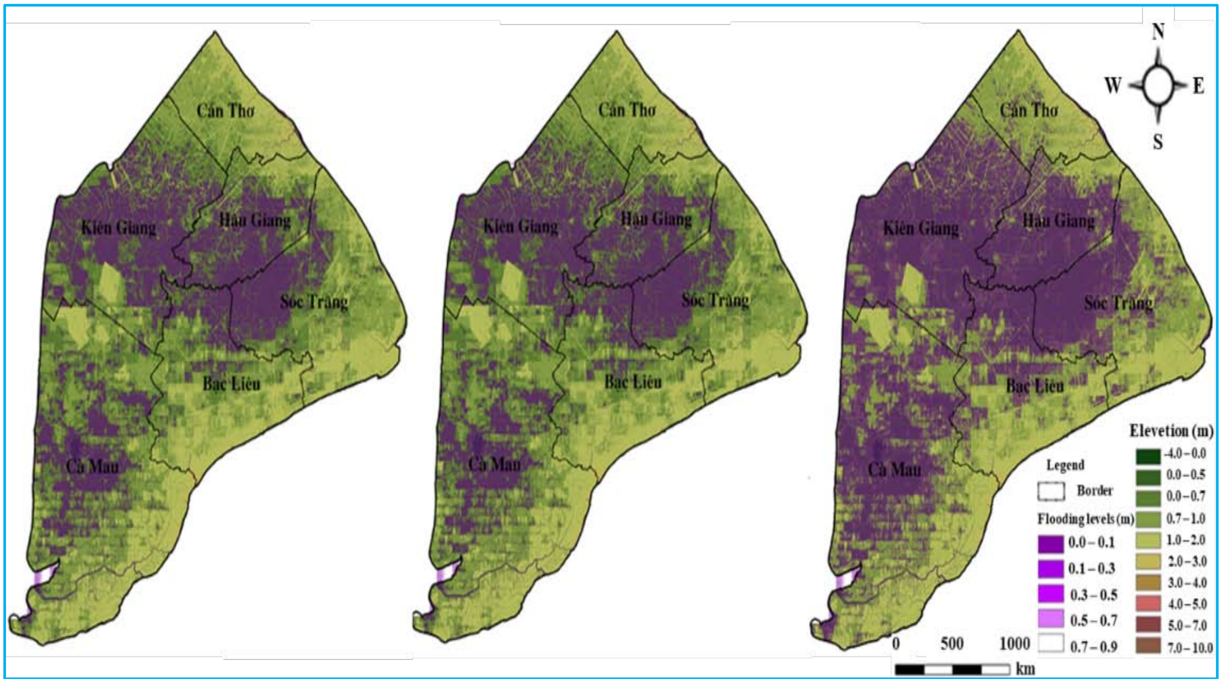

Fig. 6. Simulation results of maximum flood hazard mapping correspond to (a) current climate condition, (b) RCP4.5 scenario and (c) RCP8.5 scenario over the entire study area

rainfall events that appeared in 2018-2020 were rated because they produced noticeable flooding in the Ca Mau Peninsula. Specifically, the storm was recorded on 15 September 2018 and lasted for 120 min with a total rainfall depth of 75 mm and an average intensity of 37.5 mm h^{-1}, which corresponds to a 50-year return period. Although no significant damage was recorded, this short-term storm resulted in high flooding depth at the LCAs. The second event occurred on 10 March 2020 and lasted for 180 min with a total rainfall depth up to 82 mm and an average intensity of 27.3 mm h^{-1}, which also corresponds to a 50-year return period. In this event, the rain lasted longer than the one from 2018, with several peaks and intensities for different durations that correspond to various return periods ranging from 2 to 50 years. In contrast to the 2018 event, this rain caused severe flooding locations such as Ca Mau city, over the entire northwestern area of the area (KienGiang province) and its central area includes a part of HauGiang, Bac Lieu and Soc Trang provinces. Most houses, practicability and rice paddies in the area were flooded by the flood rainfall event.

Fig. 6 presents the maximum flood hazard mapping for both present climate and future climate scenarios corresponding to RCP4.5 and RCP8.5 scenarios over the entire study area. Fig. 6 shows that flooding depth may increase significantly in future climate scenarios due to climate variability compared to baseline.

Specifically, the maximum 1-day rainfall intensity for a 50-year return period was 164.5 mm hr-1 for the baseline period while the corresponding values of RCP4.5 and RCP8.5 scenarios were 252.4 and 264.7mm hr^{-1}, respectively. It means that the maximum 1-day rainfall intensity for a 50-year return period of RCP4.5 and RCP8.5 scenarios increased 53.4 and 60.9% compared to the baseline. The spatial distribution of flooding depths under the baseline is lower than that under future rainfall scenarios. Specifically, the results of maximum flood depth at a typical location corresponding to baseline was 0.53 cm while the corresponding values of RCP4.5 and RCP8.5 scenarios were 0.62 and 0.75 cm, respectively. It implies that the maximum flood depth at the same location may increase 16.9 and 41.5%, respectively for RCP4.5 and RCP8.5 scenarios. This conclusion agrees with previous research by Lee and Dang (2020), who reported that an increasing trend in rainfall recorded at the sub-area of the Mekong Delta and a high risk of the large-scale flood may occur across the area in the future. The flood peak depth is higher 18.2 and 43.7% in the future climate conditions compared to the baseline. In general, the simulation results show that exceed rainfall under the RCP4.5 and RCP8.5 scenarios produced higher peak depths in the same locations compared to the baseline of the same return interval.

As a limitation to this study, the impacts of land-cover and social alterations were not mentioned in this work. It is, thus, needed to consider in studies on flood hazard mapping establishment in further study.

4. Conclusions

This study established the flood hazard mapping based on simulating the rainfall intensity-duration-frequency model for the Ca Mau Peninsula of Vietnam. The flood depth mappings were constructed integrating ArcGIS software and available topographical data in the entire Ca Mau Peninsula under current rainfall and future change scenarios. The average rainfall amount for specific flood events increased around 7.2 and 12.4% for RCP4.5 and RCP8.5 scenarios compared with the baseline while the largest 1-day rainfall intensity for 50-year return period increased approximately 53.4 and 60.9% and the largest flood depth at the same location increased 16.9 and 41.5%, compared to baseline.

In general, the establishment of flood hazard mapping can be useful information to alert areas where a high potential for flooding risks in the future. The applied method is simple and provides a tool for the improvement of flood risk management methods.

Acknowledgement

This research is funded by Vietnam National University Ho Chi Minh City (VNU-HCM) under grant number C2021-18-06 project entitled "Establishing rainfall intensity-duration-frequency curves (IDF) to support urban flood warnings for Ca Mau City in the context of climate change". In addition, I wish to express my sincere thanks to the anonymous reviewers for their helpful comments, which helped me to improve this manuscript.

Disclaimer : The contents and views expressed in this research paper/article are the views of the authors and do not necessarily reflect the views of the organizations they belong to.

References

Alfieri, L., Burek, P., Feyen, L. and Forzieri, G., 2015, "Global warming increases the frequency of river floods in Europe", *Hydrol. Earth Syst. Sci*., **19**, 2247-2260.

Bathrellos, G. D., Skilodimou, H. D., Chousianitis, K., Youssef, A. M. and Pradhan, B., 2017, "Suitability estimation for urban development using multi-hazard assessment map", *Sci. Total Environ*., **575**, 119-134.

Buishand, T. A., 1982, "Some methods for testing the homogeneity of rainfall records", *J. Hydrol*., **58**, 11-27.

Courtey, L. G., Wilby, R. L., Hillier, J. K. and Slater, J., 2019, "Intensity-duration-frequency curves at the global scale", *Environ. Res. Lett*., **14**, 084045.

Dang, T. A., 2020, "Simulating rainfall IDF curve for flood warnings in the Ca Mau coastal area under the impacts of climate change", *International Journal of Climate Change Strategies and Management*, **12**, 5, 705-715.

David, A. and Schmalz, B., 2020, "Flood hazard analysis in small catchments : Comparison of hydrological and hydrodynamic approaches by the use of direct rainfall", *J. Flood Risk Manag*., e12639.

Feloni, E., Mousadis, I. and Baltas, E., 2020, "Flood vulnerability assessment using a GIS-based multi-criteria approach-The case of Attica region", *J. Flood Risk Manag*., **13**, e12563.

Ho, C. T. and Dang, T. A., 2021, "Simulating rainfall intensity-duration-frequency curve towards establishing innundation maps in Ca Mau peninsula", *Vietnam Journal of Hydrometeorology*, **727**, 33-43.

IPCC, 2019, "Summary for Policymakers", In : Climate Change and Land : An IPCC special report on climate change, desertification, land degradation, sustainable land management, food security and greenhouse gas fluxes in terrestrial ecosystems [P.R. Shukla, J. Skea, E. Calvo Buendia, V. Masson-Delmotte, H.- O. Pörtner, D. C. Roberts, P. Zhai, R. Slade, S. Connors, R. van Diemen, M. Ferrat, E. Haughey, S. Luz, S. Neogi, M. Pathak, J. Petzold, J. Portugal Pereira, P. Vyas, E. Huntley, K. Kissick, M. Belkacemi, J. Malley, (eds.)]. In press.

Komolafe, A. A., Herath, S. and Avtar, R., 2018, "Methodology to assess potential flood damages in urban areas under the influence of climate change", *Nat. Hazards Rev*., **19**, 05018001.

Lee, S. K. and Dang, T. A., 2020, "Extreme rainfall trends over the Mekong Delta under the impacts of climate change", *International Journal of Climate Change Strategies and Management*, **12**, 5, 639-652.

Madsen, H., Arnbjerg Nielsen, K. and Mikkelsen, P. S., 2009, "Update of regional intensity-duration-frequency curves in Denmark: Tendency towards increased storm intensities", *Atmos. Res*., **92**, 343-349.

Madsen, H., Lawrence, D., Lang, M., Martinkova, M. and Kjeldsen, T. R., 2014, "Review of trend analysis and climate change projections of extreme precipitation and floods in Europe", *J. Hydrol*., **519**, 3635-3650.

MNRE - Ministry of Natural Resources and Environment, 2016, "Climate change scenarios and sea level rise for Vietnam", Publishers' resources, environment and map of Vietnam.

Ouma, Y. O. and Tateishi, R., 2014, "Urban flood vulnerability and risk mapping using integrated multi-parametric AHP and GIS: Methodological overview and case study assessment", *Water*, **6**, 1515-1545.

Radwan, F., Alazba, A. A. and Mossad, A., 2019, "Flood risk assessment and mapping using AHP in arid and semiarid regions", *Acta Geophys.*, **67**, 215-229.

Skilodimou, H. D., Bathrellos, G. D. and Alexakis, D. E., 2021, "Flood hazard assessment mapping in burned and urban areas", *Sustainability*, **13**, 4455.

Termeh, S. V. R., Kornejady, A., Pourghasemi, H. R. and Keesstra, S., 2018, "Flood susceptibility mapping using novel ensembles of adaptive neuro fuzzy inference system and metaheuristic algorithms", *Sci. Total. Environ.*, **615**, 438-451.

Tsanakas, K., Gaki Papanastassiou, K., Kalogeropoulos, K., Chalkias, C., Katsafados, P. and Karymbalis, E., 2016, "Investigation of flash flood natural causes of Xirolaki Torrent, Northern Greece based on GIS modeling and geomorphological analysis", *Nat. Hazards*, **84**, 1015-1033.